

Evaluation of DFO-HOPO as an octadentate chelator for zirconium-89

L. Allott^{†a}, C. Da Pieve^{†a}, J. Meyers^b, T. Spinks^a, D. M. Ciobota^a, G. Kramer-Marek^a and G. Smith^{a*}

^a Division of Radiotherapy and Imaging, The Institute of Cancer Research, 123 Old Brompton Road, London, UK

^b Cancer Research UK Cancer Therapeutics Unit, The Institute of Cancer Research, 123 Old Brompton Road, London, UK

*Corresponding author: graham.smith@icr.ac.uk

[†] Author contributions: Equal contribution for first authorship.

The future of ⁸⁹Zr-based immuno-PET is reliant upon the development of new chelators with improved stability compared to the currently used deferoxamine (DFO). Herein, we report the evaluation of the octadentate molecule DFO-HOPO (3) as a suitable chelator for ⁸⁹Zr and a more stable alternative to DFO. The molecule showed good potential for the future development of a DFO-HOPO-based bifunctional chelator (BFC) for the radiolabelling of biomolecules with ⁸⁹Zr. This work broadens the selection of available chelators for ⁸⁹Zr in search of improved successors of DFO for clinical ⁸⁹Zr-immuno-PET.

An increasing interest in zirconium-89 (⁸⁹Zr) for preclinical and clinical immuno-positron emission tomography (PET) is owed to its favourable decay characteristics ($t_{1/2} = 78.4$ h, $\beta^+ = 22.8\%$, $E_{\beta^+max} = 901$ keV) for the radiolabelling of antibodies which have long biological half-lives.¹⁻⁴ Currently, deferoxamine (DFO) is the chelator most commonly used to radiolabel biomolecules with ⁸⁹Zr.⁵ DFT modelling showed that the coordination sphere in the Zr-DFO complex consists of the Zr⁴⁺ cation, six donor atoms belonging to the DFO molecule, and other two coordination sites being occupied by water molecules.^{6, 7} As a result of this incomplete coordination of ⁸⁹Zr by the hexadentate DFO molecule, the ⁸⁹Zr-DFO complex undergoes a certain degree of demetallation *in vivo* with the released

^{89}Zr taken up by the bone.⁸ This is of concern because bone uptake of free $^{89}\text{Zr}^{4+}$ is undesirable owing to the high radiation dose to bone marrow; furthermore this background uptake can confound image acquisition of bone malignancies such as bone metastases. To solve the instability, different strategies have been investigated. Alternative hexadentate macrocycles (i.e. Fusarinine C) and hydroxypyridinone-based compounds (i.e. CP256) have been produced and tested but showed either no improvement or poorer stability *in vivo* when compared to DFO.^{9, 10} Additionally, a variety of either linear or macrocyclic octadentate chelators have been developed with structures hinged around hydroxamic acid or hydroxypyridinone moieties which resulted in ^{89}Zr -complexes displaying either increased or decreased stability compared to DFO.¹¹⁻¹⁶ White *et al.* described the use of a DFO-1-hydroxy-2-pyridone ligand (DFO-HOPO) as an effective sequestering agent for the treatment of plutonium (IV) intoxication (Fig. 1).¹⁷ The authors showed that the addition of one 1,2-HOPO molecule to DFO produced a low toxicity octadentate chelator which yielded very stable complexes with Pu(IV) at physiological pH. Herein, we report an updated synthesis of DFO-HOPO (**3**) which was then evaluated as an octahedral ligand for ^{89}Zr . The stability of the radiocomplex was tested *in vitro* and *in vivo* and compared to ^{89}Zr -DFO in order to confirm **3** as a viable alternative to the chelators for ^{89}Zr already described in the literature.

The synthesis of DFO-HOPO (**3**) was adapted from a literature procedure.¹⁷ In brief, commercially available DFO was reacted with hydroxamic acid chloride (**2**) and the product (**3**) was isolated by semi-preparative RP-HPLC (Scheme S1). No protection of the N-hydroxyl group of **1** was necessary. To determine and characterise the coordination capabilities of the chelator, the non-radioactive $^{\text{nat}}\text{Zr}$ complex of DFO-HOPO ($^{\text{nat}}\text{Zr}$ -**3**) was prepared in macroscopic scale by mixing the chelator with ZrCl_4 at room temperature. Showing the value of 784.247 *m/z*, the high resolution mass spectrometry (HRMS) analysis of $^{\text{nat}}\text{Zr}$ -**3** confirmed the expected complex mass to indicate a metal-to-ligand binding ratio of 1:1. Examination by RP-HPLC showed the elution of $^{\text{nat}}\text{Zr}$ -**3** as a single peak at 7:20 min:sec, *ca* 33 seconds before HOPO-DFO (**3**). The coordination of the metal ion by the chelator was further confirmed by infrared spectrometry (IR) analysis which showed a red-shift in the main carbonyl stretching band from *ca* 1620 to *ca* 1600 cm^{-1} . Additional characterisation of the complex by ultraviolet-visible

spectroscopy (UV-Vis) showed no detectable difference between the absorption spectra of $^{nat}\text{Zr-3}$ and **3**. Moreover, NMR analysis of the ^{nat}Zr complex could not be performed due to its poor solubility in any solvent.

To verify the steric and electronic ability of **3** to form a Zr(IV) octadentate chelate, density functional theory (DFT) calculations were carried out. The optimised geometry (based on the lower energy conformation) shows the metal centre coordinated to eight oxygen atoms of the chelator (Fig. 2). The Zr-O bond distances were in the range of 2.14 – 2.36 Å, in agreement with values reported in the literature for similar complexes.^{11, 12} In common with $^{89}\text{Zr-DFO}$, the preparation of $^{89}\text{Zr-3}$ was performed as previously described in the literature by incubating the chelator with a neutralised ^{89}Zr solution at room temperature for 1 h (pH 7) to guarantee a quantitative (>99%) radiolabelling which could be achieved up to 20 MBq/nmol even at low concentration of the chelators (3-8 μM).¹⁸ All reactions were monitored by radioactive instant thin layer chromatography (radio-ITLC). A variety of mobile and stationary phases were tested to find the optimum analytical conditions for both $^{89}\text{Zr-3}$ and $^{89}\text{Zr-DFO}$, which was used as a comparison. The elution profiles of both the radioactive complexes were affected by the type of stationary phase employed, and only the positively charged $^{89}\text{Zr-DFO}$ (consequence of the hexadentate chelation of ^{89}Zr) was influenced also by the mobile phase pH, when SG-ITLC strips were used. The results suggest that, differently from $^{89}\text{Zr-DFO}$, $^{89}\text{Zr-3}$ is present in solution as a neutral complex, achievable through the octadentate chelation of ^{89}Zr . This finding further advocates the involvement of the 1,2-HOPO moiety of **3** in the coordination of the metal centre. Enabling the elution of $^{89}\text{Zr-3}$ and the $^{89}\text{Zr-DFO}$ as well defined and separated bands (R_f of 0.6 and 0.1 respectively on SG-ITLC strips), ammonium acetate (0.1 M, pH 7) was used as mobile phase for the ITLC analysis. Interestingly, the radio-ITLC of $^{89}\text{Zr-3}$ revealed the presence of two well-separated spots (R_f of ca 0.6 and 0.1); the relative intensity of the spots was dependent on the specific activity of the product (i.e. concentration of the chelator) and on time. By lowering the specific activities of the product, with a consequent increase of the concentration of **3**, a decrease of the band having $R_f = 0.1$ was observed. After 24 hours at ambient temperature, only the band having $R_f = 0.6$ was detected. Performing the radiolabelling reaction at 80°C reduced the quantity of the product eluting with an $R_f = 0.1$ but did not prevent it from forming. These observations

suggest that the two bands represent two different forms of the $^{89}\text{Zr-3}$ complex; an initial transitional kinetic product which converted into a final thermodynamically stable product. Examination of the chromatographic data of $^{89}\text{Zr-3}$ could help explain the phenomenon; the transitional product was detected at the origin of the radio-ITLC strip ($R_f = 0.1$ at pH 7) suggesting it was charged (similarly to hexacoordinated $^{89}\text{Zr-DFO}$), possibly as the result of incomplete coordination of the radiometal. With an $R_f = 0.6$ (at pH 7), the thermodynamically stable final product was most likely neutral, a condition which would be achieved by the complete chelation of ^{89}Zr by octadentate **3**. Moreover, radio-HPLC analysis of $^{89}\text{Zr-3}$ after 24 hours showed only one product (corresponding to the band with $R_f = 0.6$ on radio-ITLC) having an elution profile very similar to that of $^{\text{nat}}\text{Zr-3}$ suggesting a similar identity as an octadentate complex. Importantly, no ^{89}Zr was released during the transition.

The stability of $^{89}\text{Zr-3}$ was initially assessed by a simple radio-ITLC analysis using an acidic buffer (pH 2) as mobile phase. Differently from $^{89}\text{Zr-DFO}$ ($14.4 \pm 4.65\%$ radioactivity not associated with DFO), $^{89}\text{Zr-3}$ showed no demetallation as a result of the enhanced coordination of the metal centre by the octadentate ligand. To mimic what might happen *in vivo*, a challenge assay assessed the stability of $^{89}\text{Zr-3}$ to transchelation in the presence of a large excess of either EDTA or DFO (pH 7). In both challenges, $^{89}\text{Zr-3}$ showed no transchelation with $>99\%$ intact complex after 7 days (Table 1). By comparison, $^{89}\text{Zr-DFO}$ demonstrated transchelation toward EDTA with 65.5% of intact complex after 7 days (Table 1). Moreover, a complete transmetallation of $^{89}\text{Zr-DFO}$ towards **3** was achieved in a matter of hours. Further experiments aiming to test the inertness of $^{89}\text{Zr-3}$ were performed in mouse serum. With $>99\%$ intact complex after incubation at 37°C for 7 days, $^{89}\text{Zr-3}$ showed a higher stability compared to $^{89}\text{Zr-DFO}$ (90.6% intact complex) (Table 1).

PET imaging and comparative biodistribution studies were performed in healthy mice for $^{89}\text{Zr-3}$ and $^{89}\text{Zr-DFO}$. At 1 h p.i. of $^{89}\text{Zr-3}$, the radioactivity was observed mainly in the bladder and intestine; some activity was also visible in the gall bladder. At 4 and 24 h p.i., most of the residual radioactivity was in the gut. These observations indicate a rapid renal clearance together with a certain extent of a slower hepatobiliary excretion. The hydrophilicity of the complexes is an important physicochemical property which regulates their distribution, metabolism,

and elimination *in vivo*. The $\text{LogD}_{7.4}$ of neutral complex $^{89}\text{Zr-3}$ was found to be -0.87 ± 0.03 which indicates a less hydrophilic character than the positively charged $^{89}\text{Zr-DFO}$ (-3.0 ± 0.01) and can explain the clearance pathway.⁹ After 24 h, the radioactivity level was minimal therefore no additional imaging studies at longer time points were carried out. Importantly, no uptake of ^{89}Zr in the bone was observed at any time point (Fig. 3).

Corroborating the PET images, the biodistribution studies clearly showed the participation of both the renal and hepatobiliary systems in the clearance of $^{89}\text{Zr-3}$ (Fig. 4). Most of the radioactivity had already cleared through the kidneys at 1 h p.i. ($1.39 \pm 0.1\% \text{ID/g}$), while at 4h p.i. the residual activity was localised in the gut (mostly small intestine with $0.898 \pm 0.252\% \text{ID/g}$). Differently from $^{89}\text{Zr-DFO}$ ($0.93 \pm 0.11\% \text{ID/g}$ still present in the kidneys), $^{89}\text{Zr-3}$ was almost completely cleared from the body at 24 h p.i. Although the values are quite low, $^{89}\text{Zr-DFO}$ showed *ca* 10-fold higher activity accumulation in the bone than $^{89}\text{Zr-3}$ at 24 h p.i. (0.037 ± 0.002 and 0.004 ± 0.001 for $^{89}\text{Zr-DFO}$ and $^{89}\text{Zr-3}$ respectively). This phenomenon could be correlated to either the higher level of radioactivity still present in the animals injected with $^{89}\text{Zr-DFO}$ or to an improved *in vivo* stability of $^{89}\text{Zr-3}$ compared to $^{89}\text{Zr-DFO}$.

In summary, the $^{89}\text{Zr-3}$ complex exhibited improved stability compared to $^{89}\text{Zr-DFO}$ in both challenge assays and in serum; the capability and favourability of **3** to form a stable chelate was clearly demonstrated by the complete transchelation of ^{89}Zr from $^{89}\text{Zr-DFO}$ in *ca* 3 h. The *in vivo* studies showed that $^{89}\text{Zr-3}$ cleared the body *via* the renal and hepatobiliary systems. However, once conjugated to a biomolecule the pharmacokinetics of the final radioconjugate will depend mainly on the biomolecule itself. Importantly, the straightforward synthesis of **3** from the commercially available DFO is amenable to allow the synthesis of a bifunctional chelator which is currently underway in our laboratory. The promising DFO-HOPO molecule is a valuable addition to the selection of available chelators for ^{89}Zr in search of successful successors of DFO for clinical immuno-PET applications based on important characteristics such as synthesis, chelate stability and *in vivo* pharmacokinetics.

We thank Tom Burley and Steven Turnock for valuable technical help. This work was supported by the Cancer Research UK – Cancer Imaging Centre

(C1060/A16464). This report is independent research funded by the National Institute for Health Research. The views expressed in this publication are those of the authors and not necessarily those of the NHS, the National Institute for Health Research or the Department of Health.

References

1. M.A. Deri, B.M. Zeglis, L.C. Francesconi and J. S. Lewis, *Nucl. Med. Biol.*, 2013, **40**, 3-14.
2. G. Fischer, U. Seibold, R. Schirmmacher, B. Wängler and C. Wängler, *Molecules*, 2013, **18**, 6469-6490.
3. Y.W.S. Jauw, C.W. Menke-van der Houven van Oordt, O.S. Hoekstra, N.H. Hendrikse, D.J. Vugts, J.M. Zijlstra, M.C. Huisman and G. A. M. S. v. Dongen, *Front. Pharmacol.*, 2016, **7**, doi: 10.3389/fphar.2016.00131.
4. D.J. Vugts, G.W.M. Visser and G. A. M. S. v. Dongen, *Curr. Top. Med. Chem.*, 2013, **13**, 446-457.
5. G.W. Severin, J.W. Engle, R.J. Nickles and T. E. Barnhart, *Med. Chem.*, 2011, **7**, 389-394.
6. J.P. Holland, V. Divilov, N.H. Bander, P.M. Smith-Jones, S.M. Larson and J. S. Lewis, *J. Nucl. Med.*, 2010, **51**, 1293-1300.
7. J. P. Holland and N. Vasdev, *Dalton Trans.*, 2014, **43**, 9872-9884.
8. J.P. Holland, V. Divilov, N.H. Bander, P.M. Smith-Jones, S.M. Larson and J. S. Lewis, *JNM*, 2010, **51**, 1293-1300.
9. C. Zhai, D. Summer, C. Rangger, G. M. Franssen, P. Laverman, H. Haas, M. Petrik, R. Haubner and C. Decristoforo, *Mol. Pharmaceutics*, 2015, **12**, 2142-2150.
10. M. T. Ma, L. K. Meszaros, B. M. Paterson, D. J. Berry, M. S. Cooper, Y. Ma, R. C. Hiderd and P. J. Blower, *Dalton Trans.*, 2015, **44**, 4884-4900.
11. M. Patra, A. Bauman, C. Mari, C. A. Fischer, O. Blacque, D. Häussinger, G. Gasser and T. L. Mindt, *Chem. Commun.*, 2014, **50**, 11523-11525.
12. M. A. Deri, S. Ponnala, B. M. Zeglis, G. Pohl, J. J. Dannenberg, J. S. Lewis and L. C. Francesconi, *J. Med. Chem.*, 2014, **57**, 4849-4860.
13. F. Guérard, Y-S. Lee and M. W. Brechbiel, *Chem. Eur. J.*, 2014, **20**, 5584-5591.
14. D. N. Pandya, S. Pailloux, D. Tatum, D. Magda and T. J. Wadas, *Chem. Commun.*, 2015, **51**, 2301-2303.
15. S.E. Rudd, P. Roselt, C. Cullinane, R.J. Hicks and P. S. Donnelly, *Chem. Commun.*, 2016, **52**, 11889-11892.
16. J. Rousseau, Z. Zhang, G. M. Dias, C. Zhang, N. Colpo, F. Bénard and K.-S. Lin, *Bioorg. Med. Chem. Lett.*, 2017, **27**, 734-738.
17. D.L. White, P.W. Durbin, N. Jeung and K. N. Raymond, *J. Med. Chem.*, 1988, **31**, 11-18.
18. M. J W D Vosjan, L. R Perk, G. W M Visser, M. Budde, P. Jurek, G. E. Kiefer and G. A. M. S. v. Dongen, *Nat. Protoc.*, 2010, **5**, 739-743.

Figures

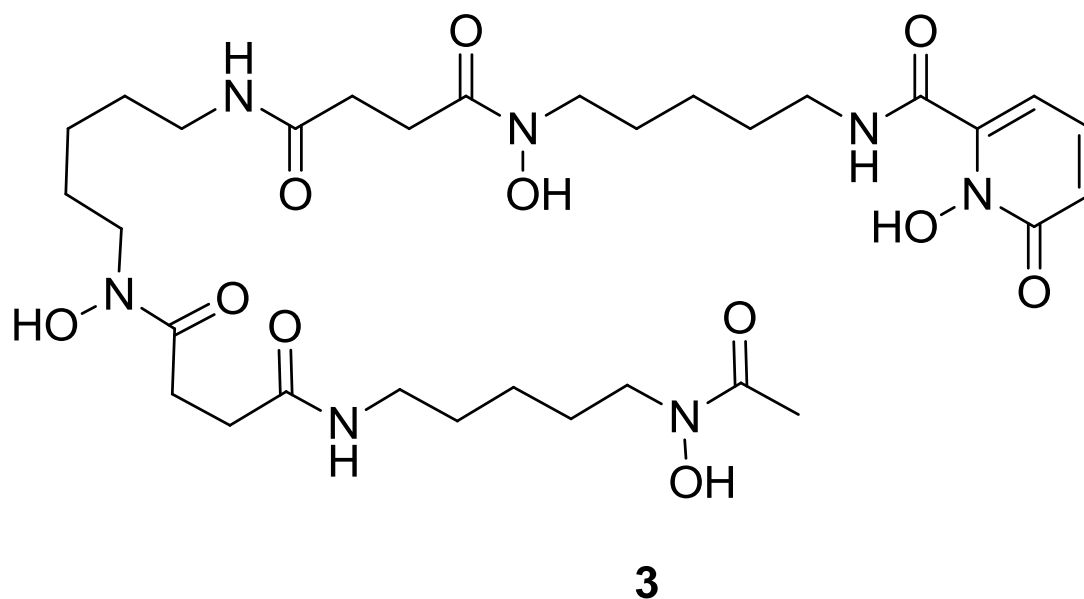


Figure 1. Structure of DFO-HOPO (**3**) containing three hydroxamic acid and one hydroxypyridone moiety for coordinating $^{89}\text{Zr}^{4+}$.

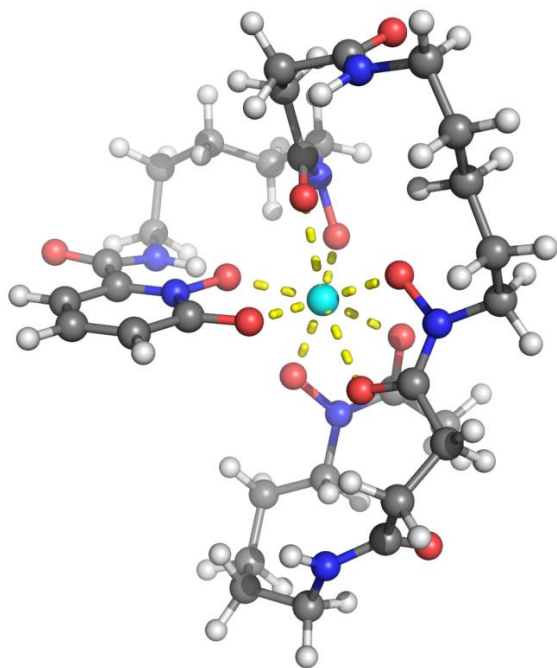


Figure 2. The DFT optimised structure of ^{89}Zr -3. (atom colour: white = hydrogen; grey = carbon; blue = nitrogen; red = oxygen; cyan = zirconium).

Complex	Competitor	Fraction of intact complex (% ± SD)						
		0 min	1 h	3 h	1 d	3 d	7 d	
A	⁸⁹ Zr-3	EDTA	>99	>99	>99	>99	>99	>99
		DFO	>99	>99	>99	>99	>99	>99
A	⁸⁹ Zr-DFO	EDTA	>99	>99	>99	75.63±3.07	63.1±0.75	65.5±4.42
		3	>99	35.8±9.8	4.1±2.35	0	0	0
B	⁸⁹ Zr-3	Mouse Serum	>99	--	>99	>99	>99	>99
	⁸⁹ Zr-DFO	Mouse Serum	>99	--	>99	97.7±0.53	94.7±0.78	90.6±1.75

Table 1. The stability of ⁸⁹Zr-3 and ⁸⁹Zr-DFO was tested against transchelation in the presence of an excess of competitor chelator over seven days (pH 7). The controls (complexes in solution without competitor) show high stability (>99% intact complex) (A). The stability of the ⁸⁹Zr-complexes was also tested in mouse serum over seven days (B).

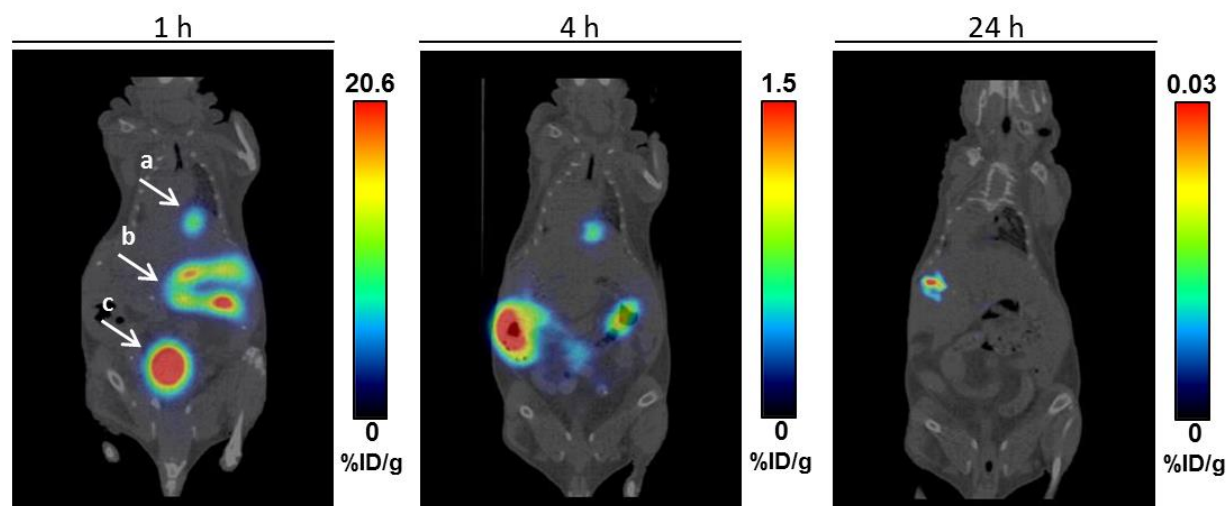


Figure 3. Coronal PET images of ⁸⁹Zr-3 in healthy mice at 1, 4 and 24 h p.i. The white arrows indicate the gall bladder (a), intestine (b) and the bladder (c). An almost complete clearance of ⁸⁹Zr-3 was observed after 24 h.

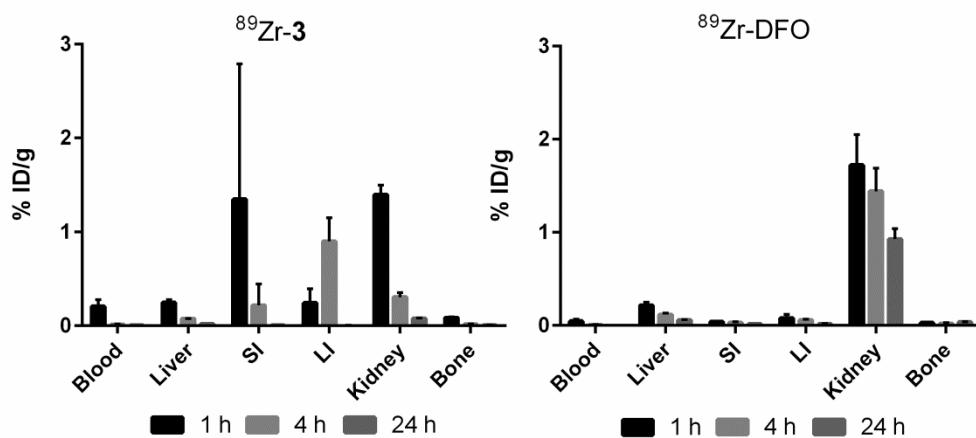


Figure 4. Biodistribution data for $^{89}\text{Zr-3}$ and $^{89}\text{Zr-DFO}$ at 1, 4 and 24 h p.i. in selected organs. SI = small intestine; LI = large intestine.